Chinese Journal of
POLYMER SCIENCE

FEATURE ARTICLE

https://doi.org/10.1007/s10118-026-3576-y
Chinese J. Polym. Sci. **2026**, *44*, 1578–1591

Advanced Light Scattering Characterization and Physics for Functional Polyelectrolyte Gels

Yu-Sen Jie[a,b] and Di Jia[a,b*]

[a] *Laboratory of Polymer Physics and Chemistry, Beijing National Laboratory for Molecular Sciences, Institute of Chemistry, Chinese Academy of Sciences, Beijing 100190, China*
[b] *University of Chinese Academy of Sciences, Beijing 100049, China*

Abstract Functional gels exhibit unique properties that can be tuned by regulating their physical interactions and microstructures. However, quantifying the strength and fraction of these physical interactions and how they result in large-scale collective dynamical properties remains a significant challenge. From this perspective, we briefly review the theories and characterization method of light scattering on polyelectrolyte gels, with an emphasis on summarizing our efforts. In particular, we introduce our most recent work on an entirely new universality class of hierarchical gel dynamics for various types of physical gels, which is complementary to the light scattering studies on chemically crosslinked gels in the past five decades. By utilizing the hierarchical gel dynamics, we are able to extract the average bond binding energy of various physical bonds and the physical crosslinking density in the gels. Finally, we evaluated the advantages and limitations of the light scattering method and discussed the future perspectives in this field. It is anticipated that this perspective will facilitate the broad application of light scattering technique in the field of functional gels.

Keywords Polyelectrolyte gel; Dynamic light scattering; Hierarchical gel dynamics; Donnan equilibrium; Swelling equilibrium

Citation: Jie, Y. S.; Jia, D. Advanced light scattering characterization and physics for functional polyelectrolyte gels. *Chinese J. Polym. Sci.* **2026**, *44*, 1578–1591.

INTRODUCTION

Gels are three-dimensional networks capable of accommodating large quantities of solvent without dissolving and exhibiting solid-like viscoelastic behavior. Biological tissues generally have gel-like properties, and are well known for their various functionalities, including lubrication, adhesive, and self-healing properties.[1–3] Extensive attention has been paid to mimicking the structures of these natural materials to endow synthetic soft materials with multifunctionality and responsiveness.[4–7] Based on the nature of the crosslinks that organize their network structure, gels can be categorized into chemical gels and physical gels. Chemical gels are formed through permanent covalent bonds, resulting in a robust and irreversible network. Poly(*N*-isopropylacrylamide),[8] poly(methacrylic acid),[9] poly(ethylene glycol) (PEG)[10] and poly(acrylamide) (PAM)[11], *etc*. are widely used in the construction of functional gels exhibiting responsiveness to temperature, light, pH and other stimuli. In contrast, physical gels are crosslinked by reversible non-covalent interactions, which encompass a broad variety of interactions such as hydrogen bond, hydrophobic interaction, ionic bond, metal-ligand coordination, and π-π stacking.[12–16] It is noted that biomacromolecules organizing into gel-like hierarchical architectures mainly rely on physical dynamic bonds,[17] thus understanding and precisely quantifying these physical dynamic bonds in gels is essential for designing the functionalities of gels.

Scattering methods are widely used to characterize the shape and structure, dynamics, moduli, and thermodynamic properties such as phase diagrams and Flory-Huggins parameters, *etc*. for polymer solution and gel systems.[18–30] Differences among three kinds of scattering techniques (neutron scattering, X-ray scattering, and light scattering) arise from how each type of radiation interacts with the samples. Neutrons interact directly with the atomic nuclei. X-ray interacts *via* electromagnetic scattering from the electron clouds of the atoms. Light interacts with materials through its polarizability and is sensitive to fluctuations of the refractive index. Along with associated parameters, such as wavelength, these factors lead to different spatial and temporal resolutions.[31] For tetra-arm PEG gels measured by small-angle neutron scattering, the longitudinal modulus measured from the zero-angle scattering intensity completely correlates with the longitudinal modulus from the swelling experiments.[32] Besides, the Flory-Huggins parameters can also be determined by measuring the zero-angle scattering intensity as a function of the volume fraction and number of monomers between crosslinks based on the Flory-Rehner theories.[33] Depending on the gel samples, the longitudinal modulus and Flory-Huggins parameters can also be measured by using dynamic and

* Corresponding author, E-mail: jiadi11@iccas.ac.cn
Special Topic: Functional Gels
Received December 22, 2025; Accepted January 14, 2026; Published online May 12, 2026

static light scattering, respectively.[34,35] Small angle X-ray scattering can probe morphology by fitting the scattering form factor $P(q)$, which arises from the interference of scattering atoms in individual chains or domains in the network.[36] For instance, microphase separation occurs in an ABA triblock copolymer gel system with end blocks, and small-angle X-ray scattering profiles can be fitted by the spherical form factor to evaluate the radius of the microphase domains.[37] Another example is that for gels with fibrillar structure, the fibril diameter can be obtained by fitting the small-angle X-ray scattering profiles using flexible cylinder model.[38]

This perspective aims to summarize our progress in the characterization of functional polyelectrolyte gels using dynamic light scattering (DLS) and static light scattering (SLS), including how to measure microscopic properties and hierarchical dynamics of gels, as well as the interplay between microscopic and macroscopic properties such as swelling behaviors. We also briefly introduce the theory and physics of charged gels. Specifically, in contrast to the rich knowledge on conventional chemical gels achieved over more than five decades, we report our most recent discovery of a new universality class of dynamics in physical gels formed by reversible and dynamic bonds. Our results show that the specific local dynamic bonding equilibria would amplify into a single hierarchical dynamical mode that is universal to all physical gels. Such physical gels are ubiquitous in a plethora of biological contexts involving protein aggregation, biomolecular condensates, and soft living matter in general, as well as in technological applications such as tissue engineering and drug delivery. Finally, the challenges and future prospects in this field are discussed. We hope such advanced light scattering characterization and physics for functional polyelectrolyte gels can be widely used in various fields to better understand the physical mechanisms of gel materials and help design better performance and functionalities in the future.

THEORY OF DYNAMIC LIGHT SCATTERING FOR POLYMER GELS

Consider a polymer gel network consisting of polymer strands and liquid medium. The gel strands undergo structural fluctuations and two modes are mainly considered in dynamic light scattering (DLS), which are the gel strands moving against the liquid medium in the form of either a longitudinal or a transverse wave.[39] Let us introduce the displacement vector $\mathbf{u}(\mathbf{r}, t)$ which represents the position $\mathbf{r}$ of a segment fluctuating around its equilibrium location at time t. The ensemble average value of $\mathbf{u}$ is zero and its divergence $\nabla\cdot\mathbf{u}$ is expressed as:[40]

$$\nabla\cdot\mathbf{u} = -\frac{\delta c}{c} \tag{1}$$

where c is the average polymer concentration, and δc is the local polymer concentration fluctuations.

When a deformation on a unit cube of the gel network with density ρ occurs, the displacement vector $\mathbf{u}$ obeys the following equation:

$$\rho\frac{\partial^2\mathbf{u}}{\partial t^2} = \nabla\cdot\sigma - f\frac{\partial\mathbf{u}}{\partial t} \tag{2}$$

The term on the left is from inertial being the mass times the acceleration of a unit cube of the gel network. The terms on the right are the forces exerted on the unit cube of the gel network. The first term represents the force of internal stress with σ being the stress tensor. The second term is from the friction of the gel network against the liquid medium with f being the friction coefficient. The value of f can be macroscopically determined by measuring the uniform velocity of the liquid flowing through the fixed gel.[39] Considering the gel network assembled by meshes with average linear size of correlation length ξ, the friction coefficient per unit volume is given as:[41]

$$f = \frac{6\pi\eta\xi}{\frac{4}{3}\pi\xi^3} = \frac{9\eta}{2\xi^2} \tag{3}$$

where η is the viscosity of the liquid medium.

Using the theory of elasticity, the relation between the stress tensor σ and displacement vector $\mathbf{u}$ is written as

$$\sigma_{ik} = K\nabla\cdot\mathbf{u}\delta_{ik} + 2\mu\left(u_{ik} - \frac{1}{3}\nabla\cdot\mathbf{u}\delta_{ik}\right) \tag{4}$$

where σ_{ik} is the component of the stress tensor, K is the bulk modulus and μ is the shear modulus. The component of the strain tensor u_{ik} is given as:

$$u_{ik} = \frac{1}{2}\left(\frac{\partial u_k}{\partial x_i} + \frac{\partial u_i}{\partial x_k}\right) \tag{5}$$

Substituting Eqs. (4) and (5) into Eq. (2), we obtain the equation of motion for the displacement vector $\mathbf{u}$:

$$\rho\frac{\partial^2\mathbf{u}}{\partial t^2} = \mu\Delta\mathbf{u} + \left(K + \frac{1}{3}\mu\right)\nabla(\nabla\cdot\mathbf{u}) - f\frac{\partial\mathbf{u}}{\partial t} \tag{6}$$

Choosing the z axis as the longitudinal direction and the elastic wave propagates along the z axis. x and y axes are the transverse directions. We denote the longitudinal component of the displacement vector $\mathbf{u}$ as u_l and transverse component as $u_\perp$. By decomposing Eq. (6) into the longitudinal and transverse components, the values of the bulk and shear moduli can be determined.[39,42] The solving analysis of Eq. (6) is as follows.

For the longitudinal component, where $\Delta\mathbf{u} = \partial^2 u_l/\partial z^2$ and $\nabla(\nabla\cdot\mathbf{u}) = \partial^2 u_l/\partial z^2$, Eq. (6) becomes[42]

$$\rho\frac{\partial^2 u_l}{\partial t^2} = \left(K + \frac{4}{3}\mu\right)\frac{\partial^2 u_l}{\partial z^2} - f\frac{\partial u_l}{\partial t} \tag{7}$$

When the friction is negligible, the longitudinal velocity is given as:

$$c_l = \sqrt{\frac{K + \frac{4}{3}\mu}{\rho}} \tag{8}$$

The sound velocity is extremely slow in gels, with the value of about 10 m/s because of the small elastic stiffness of the gels. When the inertia is negligible, from Eq. (7) we get

$$\frac{\partial u_l}{\partial t} = \frac{\left(K + \frac{4}{3}\mu\right)}{f}\frac{\partial^2 u_l}{\partial z^2} \tag{9}$$

Eq. (9) exhibits a formal analogy with the diffusion equation. Thus, the prefactor on the right-hand side of Eq. (9) is defined as the gel diffusion coefficient D_{gel},

$$D_{\text{gel}} = \frac{\left(K + \frac{4}{3}\mu\right)}{f} \equiv \frac{M}{f} \tag{10}$$

where M is the longitudinal modulus. Compared to the diffu-

sion coefficient of the polymer chain in solution $D = k_BT/6\pi\eta R_h$ (k_BT is the Boltzmann constant times the absolute temperature, R_h is the hydrodynamic radius of the chains), the gel diffusion coefficient does not imply any element experiences diffusion within the gel, but rather represents the elasticity of the gel network. Applying the Fourier transform to Eq. (9) reveals that the fluctuations of the wavevector **q** decay with a time constant $1/\tau_s = Mq_2/f$, where the longitudinal direction is defined as the direction of **q**, *i.e.*, $q = (0, 0, q)$.[39] D_{gel} is also interpreted as the cooperative diffusion coefficient due to the connection between the displacement vector and the local polymer concentration. Therefore, D_{gel} is related to the effective correlation length ξ of the monomer concentration in the gel network, analogous to that in semidilute polymer solutions:

$$D_{gel} = \frac{k_BT}{6\pi\eta\xi} \tag{11}$$

The correlation length ξ of the monomer concentration is commonly denoted as the mesh size in the literature.[43]

For the transverse component, where $\Delta\mathbf{u} = \partial^2 u_\perp/\partial z^2$ and $\nabla(\nabla\cdot\mathbf{u}) = 0$, Eq. (6) becomes[42]

$$\rho\frac{\partial^2 u_\perp}{\partial t^2} = \mu\frac{\partial^2 u_\perp}{\partial z^2} - f\frac{\partial u_\perp}{\partial t} \tag{12}$$

with the transverse velocity $c_\perp$ and the transverse gel diffusion coefficient $D_\perp$ given as $c_\perp = \sqrt{\mu/\rho}$ and $D_\perp = \mu/f$.

Dynamic light scattering measures the time correlation functions of electric field scattered by the longitudinal and transverse fluctuations using polarized and depolarized light, respectively. The electric field correlation function $\langle\mathbf{E}(\mathbf{q}, t)\cdot\mathbf{E}(\mathbf{q}, 0)\rangle$ can be obtained from Eqs. (7) and (12).[39] For polarized scattering it can be expressed as

$$\langle\mathbf{E}_{pol}(\mathbf{q}, t)\cdot\mathbf{E}_{pol}(\mathbf{q}, 0)\rangle = \frac{Ak_BT}{M}\exp\left(-\frac{M}{f}q^2t\right) \tag{13}$$

And for depolarized scattering it can be expressed as

$$\langle\mathbf{E}_{dep}(\mathbf{q}, t)\cdot\mathbf{E}_{dep}(\mathbf{q}, 0)\rangle = \frac{Bk_BT}{\mu}\exp\left(-\frac{\mu}{f}q^2t\right) \tag{14}$$

Here, A and B depend on the incident light, dielectric properties and scattering volume. When $t \ll f/Mq^2$, the scattered electric field is well-correlated.[36] The scattering wavevector q can be calculated by $q = 4\pi n\sin(\theta/2)/\lambda$, where n is the refractive index of the liquid medium, θ is the scattering angle, and λ is the wavelength of incident light. Typically, DLS measures the scattered light intensity-intensity correlation $\langle I(q, t)\cdot I(q, 0)\rangle / \langle I(q, 0)\rangle^2$, which is defined as $g_2(q, t)$. It can be converted to the electric field-field correlation function $g_1(q, t) = \langle E^*(q, t)\cdot E(q, 0)\rangle / \langle E_2(q, 0)\rangle$ using the Seigert relation[31]

$$g_2(q, t) = 1 + \gamma|g_1(q, t)|^2 \tag{15}$$

where γ is the coherence factor.

For homogeneous gels, the electric field-field correlation function $g_1(q, t)$ for the longitudinal mode decays as

$$|g_1(q, t)|^2 = \exp\left(-2D_{gel}q^2t\right) = \exp\left(-\frac{2M}{f}q^2t\right) \tag{16}$$

and $g_1(q, t)$ for the transverse mode is given by

$$|g_1(q, t)|^2 = \exp\left(-2D_\perp q^2t\right) = \exp\left(-\frac{2\mu}{f}q^2t\right) \tag{17}$$

The gel diffusion coefficient D_{gel} and the transverse gel coefficient $D_\perp$ can be determined using polarized and depolarized light scattering, respectively.

For most of the copolymerized gels, the frozen inhomogeneity appears due to the "cross-linked in" concentration fluctuations and dramatically influences the time-averaged scattered light intensity,[36] which makes the scattered light intensity space-dependent.[44] There are two methods to analyse the correlation functions: homodyne approach and heterodyne approach. Considering the unequal ensemble average of time and space respectively, the homodyne method gives the apparent diffusion coefficient D_A from the time averaged correlation function by[44]

$$D_A = \frac{1}{2q^2}\lim\frac{\partial}{\partial t}\ln[g_2(q, t) - 1] \tag{18}$$

The non-ergodic diffusion coefficient D_{NE} is related to D_A through the initial amplitude $\sigma_I^2 = g_2(q, 0) - 1$,

$$D_{NE} = \frac{\sigma_I^2}{Y}D_A \tag{19}$$

where $Y = \langle I\rangle_E/\langle I\rangle_T$ is the parameter related to the inhomogeneity and $\langle I\rangle_E$ and $\langle I\rangle_T$ are the ensemble-averaged and time-averaged intensities, respectively. D_{NE} is highly dependent on q because of q-dependence of both σ_I^2 and Y. Therefore, the q range must be chosen large enough for highly inhomogeneous gels.[36,45]

The heterodyne approach considers the scattered light intensity as a sum of the fluctuating component $\langle I\rangle_F$ and the static component $\langle I\rangle_S$. The ergodic assumption is still valid and the heterogeneity shows up as a static electric field, which interferes with the scattered electric field from the gel mode. In this case, the intensity correlation function is expressed as[46–49]

$$\begin{aligned} g_2(q, t) - 1 &= X^2[g_1(q, t)]^2 + 2X(1 - X)g_1(q, t) \\ &= 1 + \gamma\exp\left(-2D_Aq^2t\right) \end{aligned} \tag{20}$$

where $X = \langle I\rangle_F/(\langle I\rangle_S + \langle I\rangle_F)$. It has been shown that the heterodyne diffusion coefficient D_{HT} is equal to

$$D_{HT} = (2 - X)D_A = \frac{\sigma_I^2}{X}D_A \tag{21}$$

If $X = 1$, D_{HT} equals to D_A, which is obtained from the homodyne approach. While for $0 < X \ll 1$, D_{HT} is a heterodyne mode, which roughly equals to $2D_A$. D_{HT} and D_A are also denoted as the true elastic diffusion coefficient and the apparent diffusion coefficient, respectively.[49]

DYNAMIC LIGHT SACTTERING IN BIOMACROMOLECULAR SYSTEM

Naturally, many biological systems, such as mucus, extracellular matrix and vitreous humor, behave like swollen hydrogels with both chemical and physical crosslinks.[50–53] It is significant to understand the internal structures, gel strand dynamics and how they are influenced by the materials or interactions that come into contact with the biological hydrogels. Scattering technique is an indispensable tool for characterizing the microstructure and dynamic behavior of biological hydrogels. It can probe the gels in a non-invasive manner and provide statistically averaged information.[31,54] In this section, we will take the silk-hyaluronic acid composite hydrogels as an example to elu-

cidate how to use light scattering technique to study biomaterials.[52]

Hyaluronic acid (HA) is a negatively charged glycosaminoglycan that plays an essential role in embryonic development, angiogenesis, joint lubrication and structural support of biological tissues.[55] Particularly, HA is an important component of native vitreous humor which consists of roughly 400 μg/cm^3 HA.[52] Previous research found that HA chemically crosslinked with silk fibroin can facilitate tunability of degradation and mechanical properties and also maintain biocompatibility.[52,55] We have used DLS to monitor the structures of these gel composites during the aging process (Fig. 1a). For example, Fig. 1(b) shows DLS results for the gels composed of 50% silk and 50% HA after 1 day under the physiological conditions. The fitting results of the correlation functions show three diffusive modes and the corresponding diffusion coefficients are presented in Fig. 1(c).

To analyse the three relaxation modes in the silk-HA composite gel, HA gel alone and silk gel alone were characterized separately. For the HA gel alone and silk gel alone, the gel diffusion coefficients are 3.69×10^{-7} and 4.37×10^{-8} cm^2/s (Figs. 1d and 1e), which are similar to D_1 and D_2 of the silk-HA composite gel respectively. As discussed in the theory section of DLS for polymer gels, the gel diffusion coefficient is related to the longitudinal modulus of the gels. Therefore, the first relaxation mode in the composite gel arises from the elasticity of HA gel network, and the second relaxation mode arises from the elasticity of the silk gel network.[52]

Besides, we also found that the synthesis of the composite gel would be incomplete if the silk content was higher than 50%. Because the molecular weight of silk (about 170 KDa) is much lower than that of HA (900–1000 KDa), the gelation ability of silk is much lower. During the synthesis of the composite gel, the silk chains are likely to crosslink with other silk chains to form microgels. Characterizing the microgel solutions formed by silk alone at the same concentration as that in the composite gel, there is one diffusive mode with D=7.58×10^{-8} cm^2/s (Fig. 1f). However, D_3 in the gel composite is much smaller than that of the silk microgels in solution because the silk microgels are under strong confinement of the composite gel network, which exerts substantial friction on the microgels. The silk and HA network collaboratively contribute to the overall elasticity of the composite gel, and some silk chains self-crosslink to form microgels in the gel network, as schematically illustrated in Fig. 1(a). After aging for 1 month, D_1 and D_2 increase yet D_3 decreases, indicating that the gel elasticity becomes larger and the movement of silk microgels in the gel network becomes slower due to the stronger confinement.[52]

DISSOCIATION-ASSOCIATION OF WEAK BONDS IN GELS AMPLIFYING INTO UNIVERSAL LAW OF HIERARCHICAL GEL DYNAMICS

Physical dynamic bonds provide tunability of numerous advanced functionalities for soft materials, such as self-healing, recyclability and responsiveness to external stimuli. Therefore, it is imperative to quantify the bond binding energy of the physical dynamic bonds and evaluate the physical crosslinking density of the gel network. Physical dynamic bonds can constantly experience the association-dissociation dynamical process, and the characteristic relaxation time is related to the bond binding energy.[56,57] Bond binding energy can vary widely due to the differences in chemical nature even for the same type of physical bond (Fig. 2a). By investigating the dynamics of various types of physical gels with different physical bonds, a universal law of hierarchical gel dynamics has been discovered using DLS.[56] For chemically crosslinked gels, $g_1(q, t)$ is proportional to the time

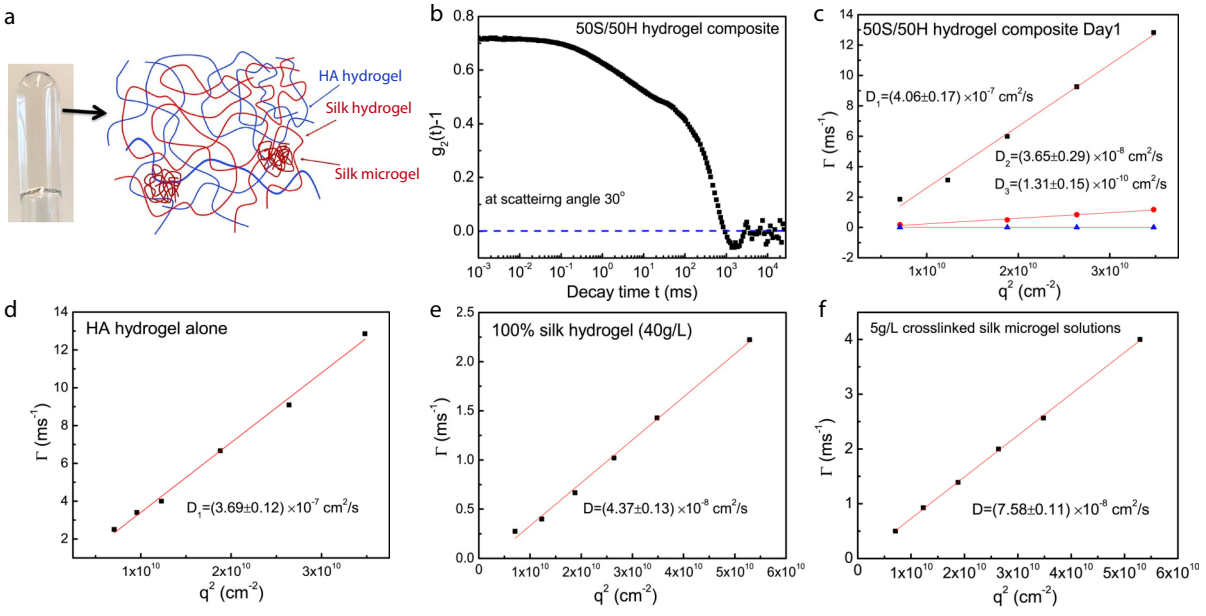

Fig. 1 (a) Schematic illustration of the silk-HA composite gel structure; (b) Correlation function $g_2(q, t)$ obtained from DLS for the silk-HA composite gel; q^2 dependence of the relaxation rates Γ for (c) silk-HA composite gel, (d) HA gel alone, (e) silk gel alone and (f) crosslinked silk microgel solutions. (Reproduced with permission from Ref. [52]; Copyright (2020), Elsevier.)

https://doi.org/10.1007/s10118-026-3576-y

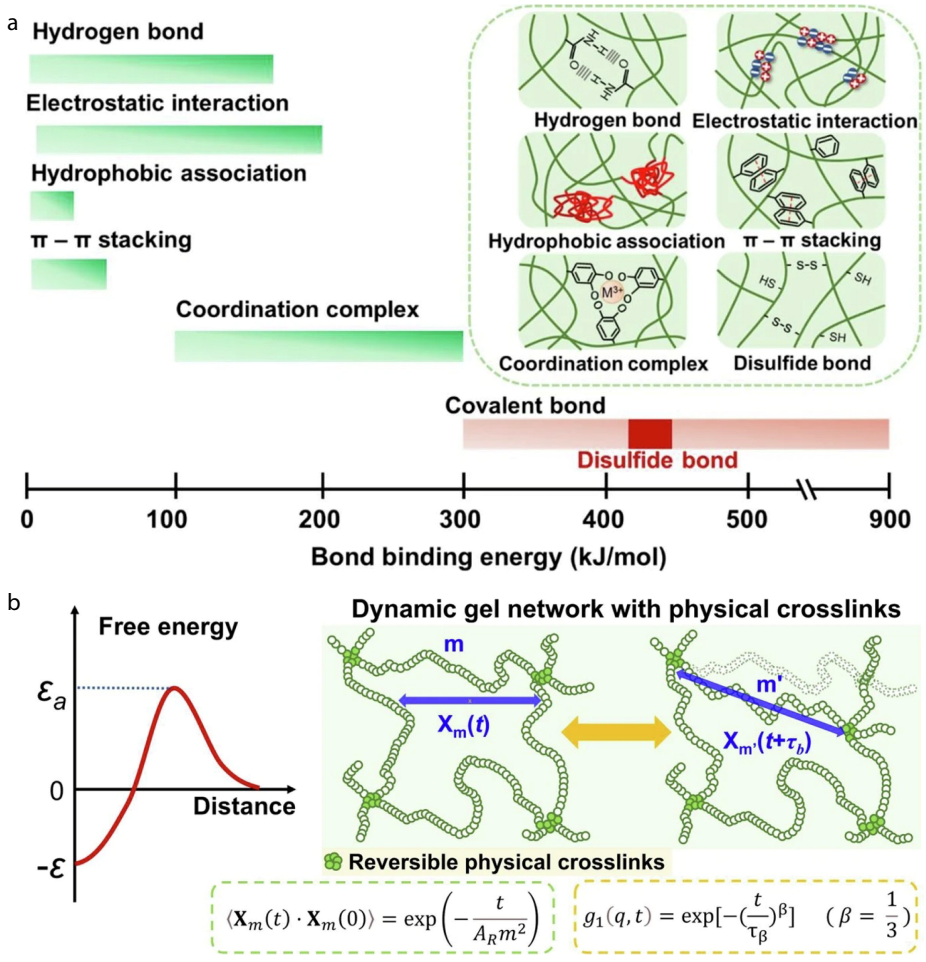

Fig. 2 (a) Bond binding energy map and schematic illustration of various physical bonds in gels; (b) Mechanism of association-dissociation hierarchical dynamics for reversible dynamic gels with physical crosslinks. The strand with m monomers and $\mathbf{X}_m(t)$ changes to m' and $\mathbf{X}_{m'}(t + \tau_b)$ after an elapse of lifetime τ_b of a physical crosslink. (Reproduced with permission from Ref. [56]; Copyright (2025), Open Access.)

correlation function of the displacement vector (denoted as $\mathbf{X}_m(t)$ in Fig. 2b) of the gel strands with m monomers between two adjacent crosslinks given by

$$g_1(q,t) \sim \langle \mathbf{X}_m(t) \cdot \mathbf{X}_m(0) \rangle \sim \exp\left(-D_{gel} q^2 t\right) \tag{22}$$

For a typical chemical gel, which is poly(acrylamide) (PAM) gel chemically crosslinked by bis-acrylamide, its correlation function $g_1(q, t)$ follows a single exponential decay with the best fitting function given at the top of Fig. 3(a). In sharp contrast, for PAM physical gel assembled through hydrogen bonds without any chemical crosslinkers, $g_1(q, t)$ exhibits an additional stretched exponential decay, representing the association-dissociation dynamical process of the physical dynamic bonds, which are hydrogen bonds (Fig. 3b). It can be fitted by one exponential decay and one stretched exponential decay, where the stretched exponent β is 1/3 (Fig. 3b). Moreover, the response of the stretched exponential mode of physical gels to the additional chemical crosslinks obey the 'one-or-none' principle. As the chemical crosslinking density increases, the fraction of the stretched exponential decay with β=1/3 gradually decreases, and when the chemical crosslinking density is above a threshold value, the stretched exponential decay disappears, indicating that it goes back to the typical feature of chemically crosslinked gels (Fig. 3c). By simply monitoring the presence/absence of the stretched exponential mode in DLS, we can identify whether physical dynamic bonds or chemical covalent bonds dominate in the gels.[56]

We tested various types of physical gels containing various physical bonds, including PAM gels assembled by hydrogen bonds, polyampholyte gels assembled by ionic bonds, and natural lysozyme fibrillar gels driven by hydrophobic associations. They all exhibited a stretched exponential decay with β=1/3 in DLS results. Besides, in Fig. 3(d), the normalized stretched exponential decay in the normalized $g_1(q, t)$ for the three types of physical gels can all be superposed into a single master curve and can be best fitted by

$$g_1(q,t) \sim \exp\left[-\left(\frac{t}{\tau_\beta}\right)^{1/3}\right] \tag{23}$$

Therefore, the local dynamic bonding equilibria can converge into a universal hierarchical dynamical mode for all types of physical gels, irrespective of their distinct chemical compositions. Moreover, the characteristic relaxation time τ_β in Eq. (23) is positively correlated with the bond binding energy. The higher bond binding energy would lead to longer characteristic relaxation time τ_β for the hierarchical gel dy-

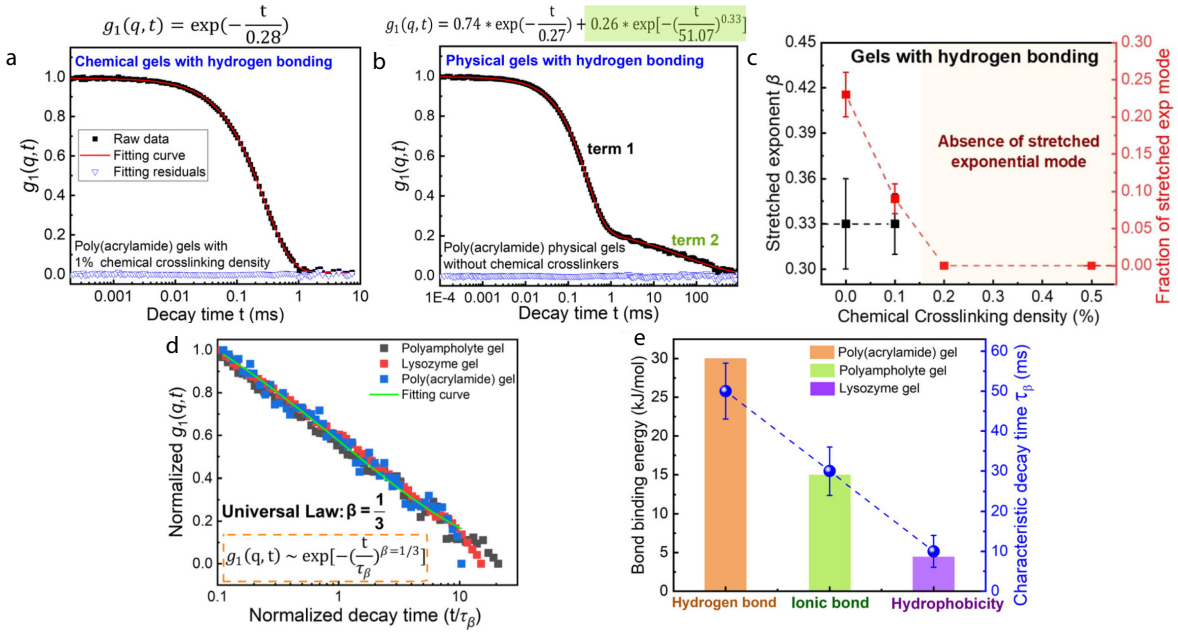

Fig. 3 (a, b) Normalized electric field correlation functions $g_1(q, t)$ for PAM gels (a) with 1% chemical crosslinking density and (b) without chemical crosslinkers; (c) Fraction of stretched exponential mode and the stretched exponent β as a plot of the chemical crosslinking density for PAM gels; (d) Superposition of the stretched exponential decay in normalized $g_1(q, t)$ as a plot against the decay time in units of the characteristic relaxation time τ_β for three types of physical gels; (e) Correlation between the measured characteristic relaxation time τ_β (filled circles, right axis) and the specific bond binding energy (bars, left axis) for three types of physical gels. (Reproduced with permission from Ref. [56]; Copyright (2025), Open Access.)

namics (Fig. 3e).[56]

We have developed a theory to better understand the origin of the universal gel dynamics.[56] We consider a system of volume V_0 containing n primary chains, each with monomer volume υ_0 and N monomers. The total number of monomer N_s capable of pairwise crosslinks is

$$N_s = fnN = f\frac{\phi_0 V_0}{\upsilon_0} \tag{24}$$

where f denotes the fraction of monomers capable of forming physical crosslinks, and ϕ_0 is the polymer volume fraction. ϵ and ϵ_a are the free energy gain and free energy barrier for the association of physical crosslinks. The rate of association k_a and the rate of dissociation k_d are $\tau_0^{-1}\exp(-\epsilon_a/k_BT)$ and $\tau_0^{-1}\exp[-(\epsilon_a+\epsilon)/k_BT]$, respectively, where τ_0 is a microscopic monomeric time scale in the range of picosecond to nanosecond, depending on the monomer friction coefficient and temperature. The average lifetime of a monomer inside a crosslink is $\tau_b=\tau_0\ \exp[(\epsilon_a+\epsilon)/k_BT]$ in the steady state. The fraction of monomers p associated into crosslinks is given using equilibrium statistical mechanics and can be expressed by[56]

$$p \approx f\phi_0\exp(\epsilon/k_BT) \tag{25}$$

The average number of pairwise crosslinks N_c per chain follows from Eqs. (24) and (25) as

$$N_c = \frac{1}{2}\frac{pN_s}{n} = \frac{1}{2}pfN = \frac{1}{2}f^2N\phi_0\exp(\epsilon/k_BT) \tag{26}$$

The physical crosslinking density ρ_c is defined as the fraction of crosslinked monomers N_c/N given by

$$\rho_c = \frac{1}{2}f^2\phi_0\exp(\epsilon/k_BT) \tag{27}$$

Specifically, m monomers in the gel strand between two adjacent crosslinks obey Poisson distribution with distribution function $P(m)$

$$P(m) = k_a\exp(-k_am) \tag{28}$$

Each strand with a particular value of m presents its chain dynamics and the internal dynamics of the physical gel is a superposition of the dynamics of all strands with various values of m. Rouse dynamics is applicable since $\phi_0 \ll 1$ so that the hydrodynamic interaction is screened and entanglement effect is weak. If the gel strands obey Gaussian chain statistics with size exponent $\nu=1/2$, the longest relaxation time τ_{Rouse} of a chain with N monomers is proportional to N^2. By drawing an analogy with a random copolymer, τ_{Rouse} of a chain with N monomers is related to the fraction of monomers in the dynamic crosslinks ρ_c and the fraction of monomers free from dynamic crosslinks $(1-\rho_c)$, as follows

$$\tau_{Rouse} = \tau_0\left[\exp\left(\frac{\epsilon+\epsilon_a}{k_BT}\right)\rho_c + (1-\rho_c)\right]N^2 \equiv A_RN^2 \tag{29}$$

where τ_0 absorbs monomer friction and temperature, and A_R is defined in Eq. (29). Based on the polymer dynamics theory, the time correlation function of the displacement vector $\mathbf{X}_m(t)$ of a Rouse strand with m monomers is

$$\langle\mathbf{X}_m(t)\cdot\mathbf{X}_m(0)\rangle \sim \exp\left(-\frac{t}{A_Rm^2}\right) \tag{30}$$

According to the DLS theory, $g_1(q, t)$ is a superposition of $\langle\mathbf{X}_m(t)\cdot\mathbf{X}_m(0)\rangle$ for each m weighted by the distribution function $P(m)$

$$g_1(q,t) \sim \int dmP(m)\langle\mathbf{X}_m(t)\cdot\mathbf{X}_m(0)\rangle \tag{31}$$

Substituting Eqs. (28) and (30) into Eq. (31) yields

$$g_1(q,t) \sim \int \mathrm{d}m \exp\left(-k_a m - \frac{t}{A_R m^2}\right) \quad (32)$$

Performing the integral with the saddle point approximation, we obtain

$$g_1(q,t) \sim \exp\left[-\left(\frac{t}{\tau_\beta}\right)^\beta\right],\ \beta = \frac{1}{3} \quad (33)$$

where

$$\tau_\beta = \frac{4\tau_0}{27}\exp\left(\frac{2\epsilon_a}{k_B T}\right)\left[\exp\left(\frac{\epsilon+\epsilon_a}{k_B T}\right)\rho_c + (1-\rho_c)\right] \quad (34)$$

Generally, for the gel strands undergoing conformational changes with the size exponent v, the Rouse relaxation time is proportional to m^{2v+1}, so that β follows as

$$\beta = \frac{1}{2v+2} \quad (35)$$

Therefore, the physical nature of such a universal law originates from the association-dissociation dynamical process of the physical dynamic bonds in physical gels. The local chemical nature of the reversible physical crosslinks is manifested in the characteristic relaxation time τ_β, which correlated with the bond binding energy. Based on Eq. (34), the physical crosslinking density ρ_c and the bond binding energy ϵ can be quantitatively determined. When the free energy gain ϵ and free energy barrier ϵ_a for the association of physical crosslinks are known from either complementary experiments or simulations, then by measuring the characteristic relaxation time τ_β in DLS, the physical crosslinking density ρ_c can be calculated. Conversely, when ϵ_a and ρ_c are known (*e.g.*, $\rho_c = 1$ for pure physical gels) and τ_β is measured in DLS, then the bond binding energy ϵ can also be calculated using Eq. (34).

It is noted that the above conclusions are valid when the gel strands obey Gaussian chain statistics. If the gel strands adopt collapsed conformation with $v = 1/3$, we can obtain $\beta = 3/8$ based on Eq. (35). To demonstrate the relation between the conformation of gel strands and the stretched exponent β, the polyampholyte (PA) gels are dialyzed against NaCl solutions with different concentrations and water to tune the strength of the ionic bonds. $g_1(q, t)$ of weakly chemically crosslinked PA gels dialyzed by 2 mol/L NaCl solution can be fitted by two diffusive modes and one non-diffusive stretched exponential mode (Fig. 4a). Besides, the diffusion coefficients of the two diffusive modes increase with increasing salt concentration c_s of the dialysis solutions (Fig. 4b). D_2 disappears at the low salt limit, yet D_1 always exists. Thus we can assign D_1 as the gel mode representing the gel elasticity, and D_2 as the "salt ion mode", which indicates the coupled motion between the counterions and co-ions with polyampholyte backbones. Such a "salt ion mode" would disappear at the low salt limit.

Another key feature is that the characteristic relaxation time τ_β decreases by almost half as the salt concentration c_s increases from 0 mol/L to 2 mol/L (Fig. 4c). This reduction is attributed to the screening of electrostatic interactions within the ionic bonds by the added salt, which accelerates the hierarchical dissociation-association relaxation of the physical crosslinks. Correspondingly, the fraction of the stretched exponential mode also decreases from 85% to 35% as c_s increases from 0 mol/L to 2 mol/L (Fig. 4c). Moreover, the conformation of the gel strands also changes with salt concentration c_s. As c_s is reduced, the electrostatic interaction is not fully screened, and hence, more oppositely charged groups in the gel strands will complex to attain the shrunken state with the size exponent $v \approx 1/3$. On the other hand, at high c_s the ionic bond is fully screened, allowing the gel strands to expand and adopt the Gaussian coil conformation ($v \approx 1/2$). based on Eq. (35), β decreases from approximately 3/8 (low salt concentration, collapsed chain conformation) to 1/3 (high salt concentration, Gaussian chain conformation), as shown in Fig. 4(d).

We further investigated the effect of the charge ratio r (number of negatively charged monomers to the total number of charged monomers) of PA gels dialyzed by water. Microscopically, at the stoichiometric charge ratio (r=0.52), the stretched exponent β reaches a maximum value of 0.38, while the gel diffusion coefficient D_{gel} reaches a minimum (Figs. 4e and 4f), indicating that the gel strands shrink at the microscopic level. Deviating from this charge balance ratio in either direction, β decreases and D_{gel} increases because unbalanced charges allow the gel strands to swell. Consistent with these microscopic findings, the macroscopic swelling ratio V/V_0 (where V_0 is the volume of the as-prepared gel and V is the gel volume after dialysis against water at swelling equilibrium) is also minimized at r=0.52 (Fig. 4e). Therefore, the macroscopic swelling ratio is consistent with the microscopic conformational change, demonstrating that at the stoichiometric charge ratio, the microscopic gel strands adopt the shrunken conformation and the macroscopic gel volume also shrinks.[56]

Our results show that the specific local dynamic bonding equilibria amplify into a single hierarchical dynamical mode that is universal to all physical gels. It is the first experimental evidence of an entirely new universal class of hierarchical dynamics for gels, despite more than five decades of DLS studies on conventional chemical gels. This discovery enables the broad use of the simple and generally available dynamic light scattering technique to quickly identify dynamic physical gels from covalently crosslinked permanent gels, quantify the local energetics of the constituent weak physical crosslinks, and implement the timing of their large-scale functional properties in a plethora of complex materials such as vitrimers and biological living materials.

SWELLING BEHAVIOR AND SCALING LAW OF POLYELECTROLYTE GELS

Consider a uniformly charged polyelectrolyte gel in polar solvent with added monovalent salt concentration c_s. Assuming that there are n gel strands, each strand contains N Kuh segments, and let N_c be the number of crosslinking points ($N_c = n/2$). We take z_p as the number of charged groups per Kuhn segment without any counterion adsorption and α as the degree of ionization considering counterion adsorption. Therefore, the counterion concentration is $\alpha z_p nN/V = \alpha z_p c$, where V is the volume of the gel and c is the monomer number concentration ($c = nN/V$). We denote the volume of the dry gel as $V_d = nN\upsilon_1$, where υ_1 is the volume of a segment. It should be noted that there are several ways to determine the values of υ_1 and N. Following the Flory-Huggins theory, υ_1 takes the same

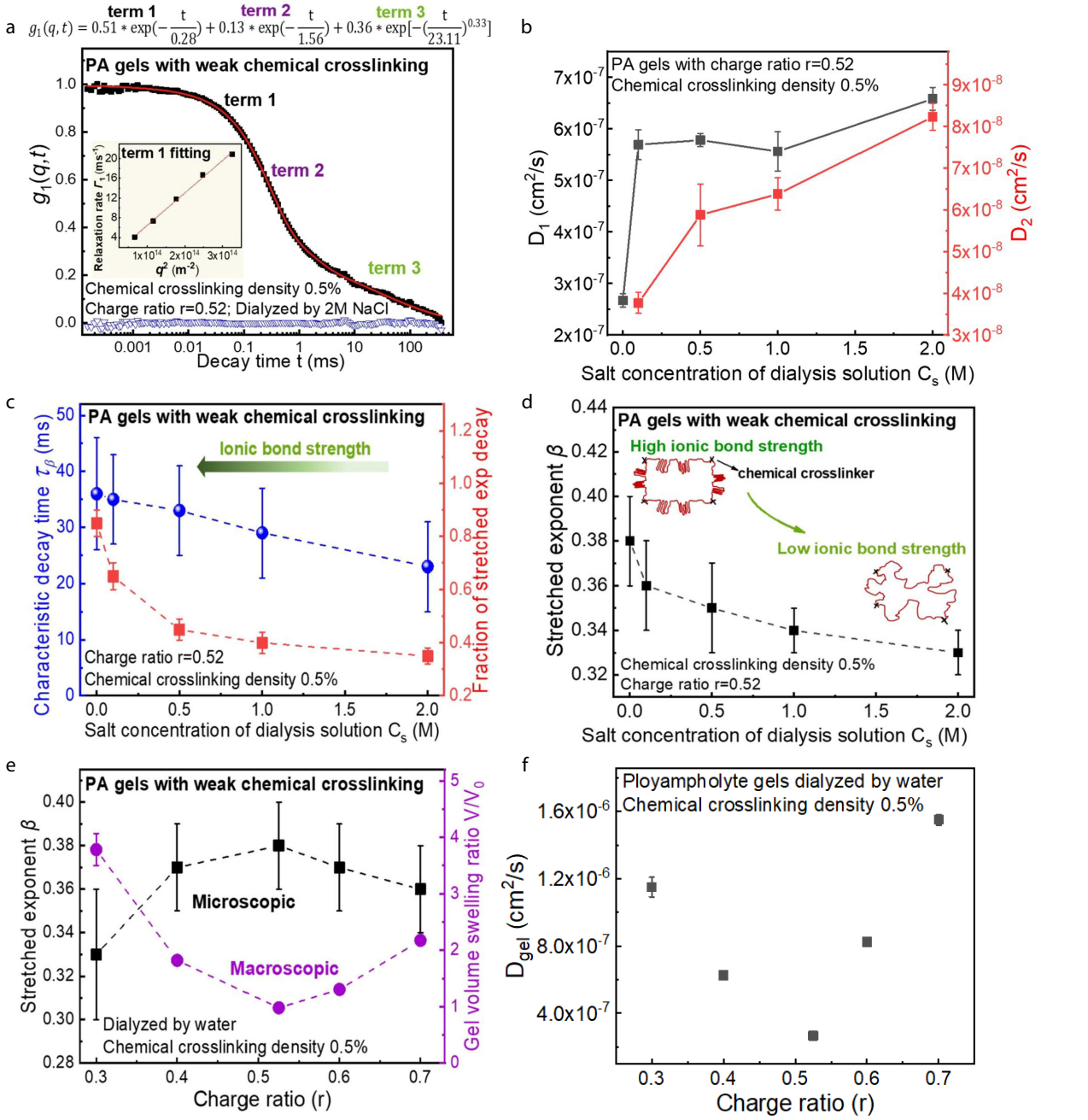

Fig. 4 (a) Correlation function $g_1(q, t)$ for weakly chemical crosslinked PA gels after dialyzed by 2 mol/L NaCl; For PA gels after dialyzing against NaCl solutions with different salt concentrations, (b) the measured diffusion coefficients D_1 and D_2, (c) characteristic relaxation time τ_β and the fraction of the stretched exponential mode, and (d) averaged stretched exponent β values. For PA gels dialyzed by water, the charge ratio dependence of (e) stretched exponent β values and macroscopic gel volume swelling ratio V/V_0, and (f) the gel diffusion coefficient D_{gel}. (Reproduced with permission from Ref. [56]; Copyright (2025), Open Access.)

value as that of the solvent molecule. The choice of υ_1 does not alter the scaling laws at the level of the monomers and solvent molecules.[41,42,49] Our model introduces a reference state in which all the gel strands obey Gaussian chain statistics. The volume fraction of the polymer in the reference state is $\phi_0 = V_d/V_0$ and that in the swollen state is $\phi = V_d/V$.

The Helmholtz free energy ΔF of the gel with Gaussian chain statistics is given as the sum of the fluctuating part and mean field part[41]

$$\Delta F = \Delta F_{\text{fluctuations}} + \Delta F_{\text{mean field}} \quad (36)$$

The first term is from the fluctuations of local polymer concentrations, conformations of the gel strands, and electrostatic correlations of small salt ions in the gels. The second term contains four parts: the free energy of mixing between the polymers and solvent, elasticity of the gels, electrostatic interactions among polymer segments and Donnan equilibrium of the electrolyte ions, expressed as

$$\Delta F_{\text{mean field}} = \Delta F_{\text{mix}} + \Delta F_{\text{elasticity}} + \Delta F_{\text{electrostatic}} + \Delta F_{\text{Donnan}} \quad (37)$$

Typically, ΔF is related to the osmotic pressure Π by Eq. (38)[43] and all the contributions to ΔF can be converted into Π, so that the osmotic pressure of the gels is the sum of the contributions from fluctuations, mixing, elasticity, electrostatic interactions and Donnan equilibrium, respectively, expressed as

$$\Pi = -\left(\frac{\partial \Delta F}{\partial V}\right)_T = \phi^2 \frac{\partial}{\partial \phi}\left(\frac{\Delta F}{V\phi}\right)_T \quad (38)$$

$$\Pi = \Pi_{\text{mix}} + \Pi_{\text{elasticity}} + \Pi_{\text{electrostatic}} + \Pi_{\text{Donnan}} + \Pi_{\text{fluctuations}} \quad (39)$$

The total osmotic pressure is zero when the gels reach swelling equilibrium. Each part is briefly introduced as follows.

The free energy of mixing n gel strands with n_1 solvent molecules is given by the Flory-Huggins theory as[58]

$$\frac{\Delta F_{\text{mix}}}{k_B T} = \frac{V}{\upsilon_1}\left[\frac{\phi}{N}\ln\phi + (1-\phi)\ln(1-\phi) + \chi\phi(1-\phi)\right] \quad (40)$$

where χ is the Flory-Huggins parameter and $1-\phi = n_1\upsilon_1/V$. Ignoring the translational entropy of the gel strands and following Eq. (38), the mixing osmotic pressure Π_{mix} is

$$\frac{\Pi_{\text{mix}}\upsilon_1}{k_B T} = -\ln(1-\phi) - \phi - \chi\phi^2 \quad (41)$$

The contribution from the elasticity of an isotropic swollen gel with stretching ratio λ is given by the rubber elasticity theory as[58]

$$\frac{\Delta F_{\text{elasticity}}}{k_B T} = \frac{3}{2}n\left(\lambda^2 - 1 - \ln\lambda\right) \quad (42)$$

Noting that $\phi_0 = V_d/V_0$, $\phi = V_d/V$, $V_d = nN\upsilon_1$ and $V = V_0\lambda^3$. Combining Eq. (38), the contribution of gel elasticity to the osmotic pressure is

$$\frac{\Pi_{\text{elasticity}}\upsilon_1}{k_B T} = -\frac{1}{N}\left(\phi_0^{2/3}\phi^{1/3} - \frac{\phi}{2}\right) \quad (43)$$

Besides, the electrostatic interaction energy is given by[41]

$$\frac{\Delta F_{\text{electrostatic}}}{k_B T} = \frac{1}{2}\frac{V}{\upsilon_1}\frac{a^2 z_p^2 \phi^2}{a z_p \phi + 2\upsilon_1 c_s} \quad (44)$$

Noting that $c_s \sim V^{-1}$, thus the osmotic pressure $\Pi_{\text{electrostatic}}$ corresponding to the electrostatic interaction is

$$\frac{\Pi_{\text{electrostatic}}\upsilon_1}{k_B T} = 0 \quad (45)$$

When the polyelectrolyte gel is soaked in salt solutions, the charges on the backbone of the polymers are confined within the gels, while the counterions and salt ions in solutions can diffuse in and out of the gel to reach the swelling equilibrium state. This state is defined as the Donnan equilibrium where the interior and exterior of the gels are charge neutral and their chemical potentials are equal. Assuming that the osmotic pressure is given by the van't Hoff law, where intermolecular interactions can be ignored, the Donnan equilibrium contribution to the osmotic pressure Π_{Donnan} is given as[41,58]

$$\frac{\Pi_{\text{Donnan}}\upsilon_1}{k_B T} = \sqrt{a^2 z_p^2 \phi^2 + 4\upsilon_1^2 c_s^2} - 2\upsilon_1 c_s \quad (46)$$

Finally, the free energy from conformational fluctuations can be obtained by drawing an analogy with a polyelectrolyte semidilute solution given by[41]

$$\frac{\Delta F_{\text{fluctuations}}}{k_B T} \approx \frac{V}{\xi^3} \quad (47)$$

The contribution of the fluctuations is significant near the critical points. Here, we restrict ourselves only to the mean field theory. Combining Eqs. (41), (43), (45) and (46), the total osmotic pressure of the gel is given by

$$\frac{\Pi\upsilon_1}{k_B T} = -\ln(1-\phi) - \phi - \chi\phi^2 - \frac{1}{N}\left(\phi_0^{2/3}\phi^{1/3} - \frac{\phi}{2}\right) + \sqrt{a^2 z_p^2 \phi^2 + 4\upsilon_1^2 c_s^2} - 2\upsilon_1 c_s \quad (48)$$

Taking $\chi = 0.4$, $\upsilon_1 = 1$ nm^3, $N = 100$, $\phi_0 = 0.1$, $a = 0.1$, $z_p = 1$ and $c_s = 0.1$ mol/L as a model gel system, the osmotic pressure of the swelling gel is shown in Fig. 5(a). Moreover, Fig. 5(b) shows that the osmotic pressure of the charged gel is always higher than that of the uncharged gel, which is mainly due to the Donnan contribution.

As mentioned above, the swelling equilibrium for isotropic swollen gels satisfies the equation in terms of ϕ, a, χ, N and c_s. Next, we proceed the derivation of the limiting behaviors in the high salt limit, and combine the experimental data to extract the scaling laws between the macroscopic and microscopic properties.

At swelling equilibrium we have $\Pi = 0$, for high salt limit with $2\upsilon_1 c_s \gg a z_p \phi$, $\phi \ll 1$, the polymer volume fraction can be calculated from Eq. (48) as[49]

$$\phi^{5/3} = \frac{\phi_0^{2/3}}{N\left(\frac{1}{2} - \chi + \frac{1}{4}\frac{a^2 z_p^2}{\upsilon_1 c_s}\right)} \quad (49)$$

To decouple the polymer volume fraction from the salt

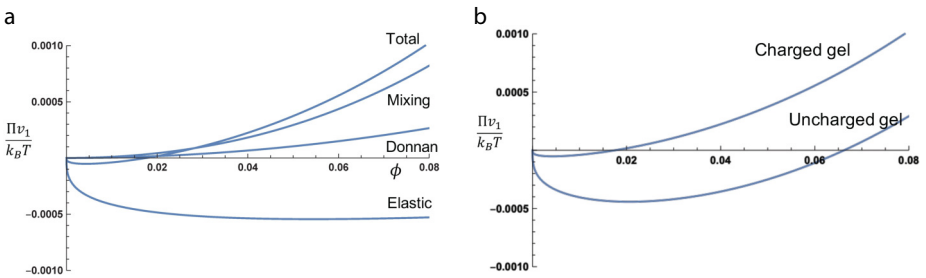

Fig. 5 (a) Contributions from mixing, Donnan equilibrium and elasticity to the total osmotic pressure; (b) Comparison between the osmotic pressure of the charged gel and uncharged gel. The parameters in (a) and (b) are $\chi = 0.4$, $\upsilon_1 = 1$ nm^3, $N = 100$, $\phi_0 = 0.1$, $a = 0.1$, $z_p = 1$ and $c_s = 0.1$ mol/L. (Reproduced with permission from Ref. [41]; Copyright (2021), Open Access.)

concentration and degree of ionization, we determine ϕ experimentally by measuring the swelling ratio of poly(acrylamide-*co*-acrylate) (PAM-PAA) gels with fixed charge density and different crosslinking densities in 0.01 mol/L NaCl solutions[49]. The volume fraction ϕ increases with an increase in the crosslinking density of the gels (Fig. 6a).

Following Eqs. (48) and (49) for high salt limit and using the theory of elasticity, the bulk modulus and shear modulus of the gels are given as[41,49]

$$K = \frac{5k_BT}{3v_1}\left(\frac{1}{2} - \chi + \frac{1}{4}\frac{a^2 z_p^2}{v_1 c_s}\right)\phi^2 \tag{50}$$

$$\mu = \frac{k_BT}{v_1}\left(\frac{1}{2} - \chi + \frac{1}{4}\frac{a^2 z_p^2}{v_1 c_s}\right)\phi^2 \tag{51}$$

Note that the bulk modulus and shear modulus of the gels are both proportional to the square of the gel volume fraction at high salt concentrations. The scaling law between the shear modulus and volume fraction has been experimentally verified, χ and a can be obtained from the intercept and slope of the linear fit.[49] By measuring the flow rate of water across the gel under a fixed pressure, the friction coefficient between the gels and the solvent can be determined. The volume fraction dependence of the friction coefficient follows the scaling law of $f \sim \phi^{4/3}$. Combined with Eqs. (10), (50) and (51), D_{gel} also follows the scaling law of $D_{gel} \sim \phi^{2/3}$.

On the other hand, if the conformational fluctuations dominate the free energy of the gel over the mean field component, Eq. (36) becomes

$$\Delta F \approx k_BT\frac{V}{\xi^3} \tag{52}$$

Thus, the osmotic pressure and bulk modulus are given by

$$\Pi \sim \frac{T}{\xi^3} \tag{53}$$

$$K = \phi\left(\frac{\partial \Pi}{\partial \phi}\right)_T \sim \frac{T}{\xi^3} \tag{54}$$

Since the shear modulus μ is proportional to the bulk modulus K, D_{gel} is given as

$$D_{gel} = \frac{M}{f} \sim \frac{T}{\eta\xi} \tag{55}$$

The correlation length ξ can be measured using static light scattering and the Ornstein-Zernike equation, as shown in Fig. 6(b).

$$I(q) = \frac{I(q \to 0)}{1 + q^2\xi^2} \tag{56}$$

The relation between ξ and ϕ can be deduced from Eqs. (50) and (54) given as

$$\xi \sim \left(\frac{1}{2} - \chi + \frac{1}{4}\frac{a^2 z_p^2}{v_1 c_s}\right)^{-1/3}\phi^{-2/3} \tag{57}$$

The experimental data in Fig. 6(c) verify the scaling law of $\xi \sim \phi^{-2/3}$ within the error bars. Moreover, Fig. 7(a) shows a typical correlation function of a polyelectrolyte gel. The correlation function $g_1(q, t)$ can be fitted by two exponential decays. The dominant mode is diffusive, because the relaxation rates Γ_1 at all angles are proportional to q^2. The other mode does not have angle dependence due to the nonergodic inhomogeneities in the gels. We can get the true elastic gel diffusion coefficient D_{gel} and apparent diffusion coefficient D_A from heterodyne and homodyne fitting, respectively (Fig. 7b). Substituting Eqs. (3), (50) and (51) into Eq. (10), D_{gel} in high salt limit is

$$D_{gel} \sim \frac{T}{\eta}\left(\frac{1}{2} - \chi + \frac{1}{4}\frac{a^2 z_p^2}{v_1 c_s}\right)^{1/3}\phi^{2/3} \tag{58}$$

Based on Eq. (58), D_{gel} decreases with c_s and follows the scaling law of $D_{gel} \sim \phi^{2/3}$. These trends are experimentally observed in Figs. 7(c) and 7(d).

The mean field theory is remarkably applicable to the polyelectrolyte gel system by considering the free energy of the gel as the sum of the free energy of mixing, elasticity, electrostatic interactions among the segments and Donnan equilibrium of electrolyte ions. Several microscopic and macroscopic parameters are expressed as closed-form equations, and the related scaling laws are consistent with the experimental results. However, when the gel approaches the critical boundary for the phase transition or the charge regularization effect is prominent, deviations of the above scaling laws are expected.

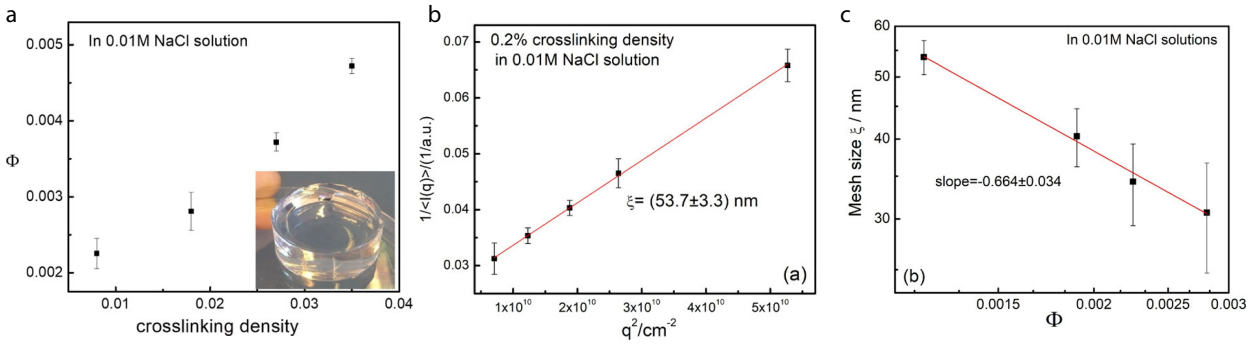

Fig. 6 (a) Volume fraction of PAM-PAA gels with 10% charge density as a function of crosslinking density in 0.01 mol/L NaCl solution. Inset is a picture of a piece of PAM-PAA gel with 10% charge density and 3.5% crosslinking density. (b) Ornstein-Zernike plot for gels with 0.2% crosslinking density and 10% charge density in 0.01 mol/L NaCl solution to obtain the gel mesh size; (c) Double-logarithmic plot of the gel mesh size ξ as a function of the gel volume fraction. (Reproduced with permission from Ref. [49], Copyright (2019), American Chemical Society.)

https://doi.org/10.1007/s10118-026-3576-y

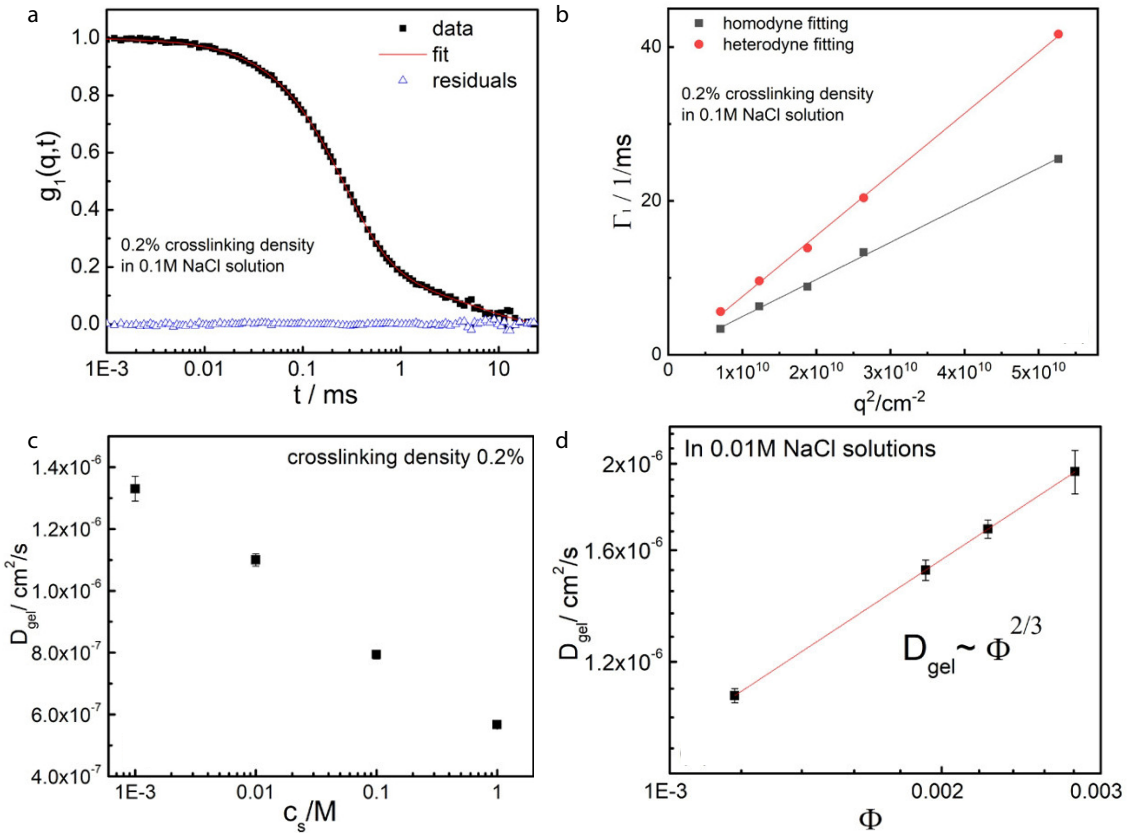

Fig. 7 (a) The normalized electric field correlation function $g_1(q, t)$ and its fitting curve with fitting residuals for gels with 0.2% crosslinking density in 0.1 mol/L NaCl solution; (b) Corresponding q^2 dependence of relaxation rates Γ_1 for gels with 0.2% crosslinking density in 0.1 mol/L NaCl solution by using both homodyne and heterodyne fitting; (c) Gel diffusion coefficient D_{gel} at different salt concentration c_s; (d) Gel diffusion coefficient D_{gel} as a function of gel volume fraction in 0.01 mol/L NaCl solution. (Reproduced with permission from Ref. [49], Copyright (2019), American Chemical Society.)

CONCLUSIONS AND PERSPECTIVES

This perspective introduces the theories and principles of light scattering techniques for the characterization of polymer gels. We can obtain the gel diffusion coefficient D_{gel} by measuring the correlation function, which originates from the displacement fluctuations of the gel strands and represents the longitudinal modulus of the gels. Then we discuss the inhomogeneity of the gel network. DLS is a powerful tool for distinguishing and decomposing this static structure contribution from the dynamic part. Dynamic light scattering works well in complicated gel systems, such as the biological gel system (silk-HA composite gel, lysozyme fibrillar gel, *etc.*) and hybrid gels containing both chemical and physical crosslinks. For physical gels, we discovered the first experimental evidence of an entirely new universal class of hierarchical dynamics. In such hierarchical dynamics, the fluctuations in elasticity and polymer concentration decay with time as a stretched exponential with exponent β=1/3 for all physical gels, and the characteristic time τ_β is a measure of the local energetics in the physical crosslinks. In contrast, in chemical gels, these fluctuations decay with time as pure exponential decays. This new hierarchical gel dynamics provides a simple and general characterization method by DLS to quickly distinguish dynamic reversible gels from permanently crosslinked gels. It can also quantify the local energetics of the constituent weak physical crosslinks, enabling a clock for their large-scale functional properties in a plethora of complex materials, such as vitrimers and biological living materials. Furthermore, a modified mean field theory can be applied to polyelectrolyte gels. The total free energy is a sum of the free energies of mixing, elasticity, electrostatic interaction and Donnan equilibrium. The theoretical predictions are in agreement with the independently measured microscopic and macroscopic quantities, and we extract scaling laws among these quantities. However, dynamic light scattering techniques face several challenges when applied to gel systems. For example, the incident light cannot pass through opaque gel samples, so that DLS measurements cannot be used. In addition, the structural heterogeneity of the gels complicates the ensemble averaging and interpretation of correlation functions. These issues can be partially solved using index matching and spatial averaging, *etc*. To overcome these inherent limitations of dynamic light scattering techniques, other methods can also be employed, such as X-ray photon correlation spectroscopy (XPCS) and neutron spin echo (NSE) spectroscopy. XPCS provides access to slow nanoscale dynamics and is less affected by the optical opacity. However, XPCS is limited by radiation damage, particularly in biological systems. NSE spectroscopy can characterize segmental polymer dynamics over nanometer length scales and nanosecond timescales with minimal radiation damage, but it requires isotopic contrast between the polymer and solvent molecules. Overall, suitable techniques can be chosen based on the specif-

ic requirements for the gel samples. Moreover, there are also several theoretical issues needed to be addressed in the future. For example, when the gel approaches the critical boundaries of the phase transition, the contributions from fluctuations would become more significant to the free energy, so that the theory needs to be modified. Future investigations are also needed to verify the generalizability of these developed theories for various types of gels, including vitrimers. We look forward to broad applications of dynamic light scattering in gel systems. It is anticipated to promote the design of gel functional properties such as gel adhesion, phase transition in 3D printing, and memory in water-based memristors, as well as mimic excellent properties in a large variety of complex gel materials.

BIOGRAPHY

Di Jia received her B.S. degree from Beijing University of Chemical Technology in 2011, and her Ph.D. degree from the Institute of Chemistry, Chinese Academy of Sciences with Professor Charles C. Han in 2016. She was a postdoctoral fellow at the University of Massachusetts Amherst with Professor Murugappan Muthukumar from 2016 to 2020. From May to August 2019, she was also a visiting scholar at the University of Freiburg in Germany with Professor Günter Reiter. She has been a professor at the Institute of Chemistry, Chinese Academy of Sciences since 2021. Currently, she leads a research group dedicated to the fundamental physics of charged soft matter including charged hydrogels, polyzwitterions, complex coacervates and biomolecular condensates *etc.* by mainly using light/X-ray/neutron scattering techniques, combined with theory. She has also utilized the discoveries in fundamental polymer physics to better design and understand life science, complex fluids, and soft living matter.

Conflict of Interests

The authors declare no interest conflict.

ACKNOWLEDGMENTS

This work was financially supported by the National Natural Science Foundation of China (Nos. W2511011 and 22273114), the Strategic Priority Research Program of the Chinese Academy of Sciences (No. XDB0770101), and International Partnership Program of the Chinese Academy of Sciences (No. 027GJHZ2022061FN).

REFERENCES

1 Seror, J.; Merkher, Y.; Kampf, N.; Collinson, L.; Day, A. J.; Maroudas, A.; Klein, J. Articular cartilage proteoglycans as boundary lubricants: structure and frictional interaction of surface-attached hyaluronan and hyaluronan–aggrecan complexes. *Biomacromolecules* **2011**, *12*, 3432–3443.
2 Nagahama, K.; Aoyama, S.; Ueda, N.; Kimura, Y.; Katayama, T.; Ono, K. Biological Tissue-inspired living self-healing hydrogels based on cadherin-mediated specific cell–cell adhesion. *ACS Macro Lett.* **2021**, *10*, 1073–1079.
3 Deng, T.; Gao, D.; Song, X.; Zhou, Z.; Zhou, L.; Tao, M.; Jiang, Z.; Yang, L.; Luo, L.; Zhou, A.; Hu, L.; Qin, H.; Wu, M. A natural biological adhesive from snail mucus for wound repair. *Nat. Commun.* **2023**, *14*, 396.
4 Ahn, S.-k.; Kasi, R. M.; Kim, S. C.; Sharma, N.; Zhou, Y. Stimuli-responsive polymer gels. *Soft Matter* **2008**, *4*, 1151–1157.
5 Matsuda, T.; Kawakami, R.; Namba, R.; Nakajima, T.; Gong, J. P. Mechanoresponsive self-growing hydrogels inspired by muscle training. *Science* **2019**, *363*, 504–508.

Graphical Abstract

Advanced Light Scattering Characterization and Physics for Functional Polyelectrolyte Gels

Yu-Sen Jie and Di Jia

Institute of Chemistry, Chinese Academy of Sciences; University of Chinese Academy of Sciences

Light scattering is a powerful technique for characterizing the elasticity, microstructures and dynamics of various functional hydrogels. The average bond binding energy and lifetime of the physical crosslinks in gel networks can also be extracted from dynamic light scattering characterization results.

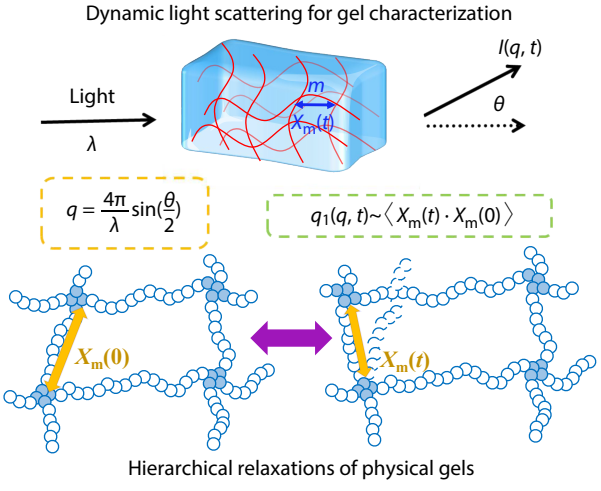

Chinese J. Polym. Sci. 2026, 44, 1578–1591 *https://doi.org/10.1007/s10118-026-3576-y*

6 Yu, C.; Guo, H.; Cui, K.; Li, X.; Ye, Y. N.; Kurokawa, T.; Gong, J. P. Hydrogels as dynamic memory with forgetting ability. *Proc. Natl. Acad. Sci. U. S. A.* **2020**, *117*, 18962–18968.
7 Echeverria, C.; Fernandes, S. N.; Godinho, M. H.; Borges, J. P.; Soares, P. I. P. Functional stimuli-responsive gels: hydrogels and microgels. *Gels* **2018**, *4*, 54.
8 Lanzalaco, S.; Armelin, E. Poly(N-isopropylacrylamide) and copolymers: a review on recent progresses in biomedical applications. *Gels* **2017**, *3*, 36.
9 Puranik, A. S.; Pao, L. P.; White, V. M.; Peppas, N. A. Synthesis and characterization of pH-responsive nanoscale hydrogels for oral delivery of hydrophobic therapeutics. *Eur. J. Pharm. Biopharm.* **2016**, *108*, 196–213.
10 Rastogi, S. K.; Anderson, H. E.; Lamas, J.; Barret, S.; Cantu, T.; Zauscher, S.; Brittain, W. J.; Betancourt, T. Enhanced release of molecules upon ultraviolet (UV) light irradiation from photoresponsive hydrogels prepared from bifunctional azobenzene and four-arm poly(ethylene glycol). *ACS Appl. Mater. Interfaces* **2018**, *10*, 30071–30080.
11 Miyata, T.; Asami, N.; Okawa, K.; Uragami, T. Rapid response of a poly(acrylamide) hydrogel having a semi-interpenetrating polymer network structure. *Polym. Adv. Technol.* **2006**, *17*, 794–797.
12 Israelachvili, J.; Pashley, R. The hydrophobic interaction is long range, decaying exponentially with distance. *Nature* **1982**, *300*, 341–342.
13 Small, D.; Zaitsev, V.; Jung, Y.; Rosokha, S. V.; Head-Gordon, M.; Kochi, J. K. Intermolecular π-to-π bonding between stacked aromatic dyads. Experimental and theoretical binding energies and near-IR optical transitions for phenalenyl radical/radical versus radical/cation dimerizations. *J. Am. Chem. Soc.* **2004**, *126*, 13850–13858.
14 Sun, T. L.; Kurokawa, T.; Kuroda, S.; Ihsan, A. B.; Akasaki, T.; Sato, K.; Haque, M. A.; Nakajima, T.; Gong, J. P. Physical hydrogels composed of polyampholytes demonstrate high toughness and viscoelasticity. *Nat. Mater.* **2013**, *12*, 932–937.
15 Sun, Z.; Lyu, F.; Wu, S.; Lu, Z.; Cheng, H. Ultrafast construction of partially hydrogen-bonded metal-hyaluronan networks with multiple biotissue-related features. *Carbohydr. Polym.* **2022**, *295*, 119852.
16 Li, H.; Chng, C. B.; Zheng, H.; Wu, M. S.; Bartolo, P. J. D. S.; Qi, H. J.; Tan, Y. J.; Zhou, K. Self-healable and 4D printable hydrogel for stretchable electronics. *Adv. Sci.* **2024**, *11*, 2305702.
17 Freeman, R.; Han, M.; Álvarez, Z.; Lewis, J. A.; Wester, J. R.; Stephanopoulos, N.; McClendon, M. T.; Lynsky, C.; Godbe, J. M.; Sangji, H.; Luijten, E.; Stupp, S. I. Reversible self-assembly of superstructured networks. *Science* **2018**, *362*, 808–813.
18 Jia, D.; Muthukumar, M. Effect of salt on the ordinary–extraordinary transition in solutions of charged macromolecules. *J. Am. Chem. Soc.* **2019**, *141*, 5886–5896.
19 Jia, D.; Muthukumar, M. Dipole-driven interlude of mesomorphism in polyelectrolyte solutions. *Proc. Natl. Acad. Sci. U. S. A.* **2022**, *119*, e2204163119.
20 Zhou, C.; Wang, Y.; Muthukumar, M.; Zhang, R.; Zhao, J.; Jia, D. Extraordinary temperature dependence of hierarchically assembled macromolecular structures with memory. *Macromolecules* **2022**, *55*, 8133–8142.
21 Jia, D.; Yang, J.-f.; Cheng, H.; Han, C. C. Basic principle of SLS/DLS measurements in fluorescent/phosphorescence solutions. *Acta Polymerica Sinica* (in Chinese) **2015**, *5*, 564–570.
22 Jia, D.; Muthukumar, M.; Cheng, H.; Han, C. C.; Hammouda, B. Concentration fluctuations near lower critical solution temperature in ternary aqueous solutions. *Macromolecules* **2017**, *50*, 7291–7298.
23 Yang, Y.; Jia, D. Phase behaviors of charged macromolecules in aqueous solutions. *Macromol. Chem. Phys.* **2023**, *224*, 2300155.
24 Wang, G. K.; Yang, Y. M.; Jia, D. Programming viscoelastic properties in a complexation gel composite by utilizing entropy-driven topologically frustrated dynamical state. *Nat. Commun.* **2024**, *15*, 3569.
25 Zhao, Y. H.; Wang, G. K.; Jia, D. Tailoring swelling ratio of smart hydrogels by utilizing entropy-driven topologically correlated structures. *Small* **2025**, *21*, e08808.
26 Jia, D.; Muthukumar, M. Electrostatically driven topological freezing of polymer diffusion at intermediate confinements. *Phys. Rev. Lett.* **2021**, *126*, 057802.
27 Jia, D.; Muthukumar, M. Topologically frustrated dynamics of crowded charged macromolecules in charged hydrogels. *Nat. Commun.* **2018**, *9*, 2248.
28 Jia, D.; Tsuji, Y.; Shibayama, M.; Muthukumar, M. Topologically frustrated dynamical state of polymers trapped in ideal uniform tetra-PEG gels. *Macromolecules* **2023**, *56*, 9389–9397.
29 Huo, L.-J.; Qu, K.-R.; Yang, Z.-Z.; Jia, D. Dynamics of charged ring polymers under gel confinement. *Chinese J. Polym. Sci.* **2025**, *43*, 399–405.
30 Jia, D.; Muthukumar, M. Dynamics of charged macromolecules under confinement. *Acta Polymerica Sinica* (in Chinese) **2023**, *54*, 151–165.
31 Han, C. C.; Akcasu, A. Z. in *Scattering and dynamics of polymers: seeking order in disordered systems*, John Wiley & Sons, **2011**, p. 36–78.
32 Horkay, F.; Nishi, K.; Shibayama, M. Decisive test of the ideal behavior of tetra-PEG gels. *J. Chem. Phys.* **2017**, *146*, 164905.
33 Matsunaga, T.; Sakai, T.; Akagi, Y.; Chung, U.-i.; Shibayama, M. Structure Characterization of tetra-PEG gel by small-angle neutron scattering. *Macromolecules* **2009**, *42*, 1344–1351.
34 Morozova, S.; Muthukumar, M. Elasticity at swelling equilibrium of ultrasoft polyelectrolyte gels: comparisons of theory and experiments. *Macromolecules* **2017**, *50*, 2456–2466.
35 Soni, V. K.; Stein, R. S. Light scattering studies of poly(dimethylsiloxane) solutions and swollen networks. *Macromolecules* **1990**, *23*, 5257–5265.
36 Morozova, S.; Hitimana, E.; Dhakal, S.; Wilcox, K. G.; Estrin, D. Scattering methods for determining structure and dynamics of polymer gels. *J. Appl. Phys.* **2021**, *129*, 071101.
37 Mischenko, N.; Reynders, K.; Koch, M. H. J.; Mortensen, K.; Pedersen, J. S.; Fontaine, F.; Graulus, R.; Reynaers, H. Small-angle X-ray and neutron scattering from bulk and oriented triblock copolymer gels. *Macromolecules* **1995**, *28*, 2054–2062.
38 Morozova, S.; Coughlin, M. L.; Early, J. T.; Ertem, S. P.; Reineke, T. M.; Bates, F. S.; Lodge, T. P. Properties of chemically cross-linked methylcellulose gels. *Macromolecules* **2019**, *52*, 7740–7748.
39 Tanaka, T.; Hocker, L. O.; Benedek, G. B. Spectrum of light scattered from a viscoelastic gel. *J. Chem. Phys.* **1973**, *59*, 5151–5159.
40 Landau, L. D.; Lifshitz, E. M. *Theory of elasticity*, Pergamon Press, Oxford, **1986**, p. 1–37.
41 Jia, D.; Muthukumar, M. Theory of charged gels: swelling, elasticity, and dynamics. *Gels* **2021**, *7*, 49.
42 Muthukumar, M. in *Physics of Charged Macromolecules: Synthetic and Biological Systems*, Cambridge University Press, Cambridge, **2023**, p. 403–411.
43 Gennes, P.-G. d. in *Scaling concepts in polymer physics*, Cornell University Press, Ithaca, N.Y., **1979**, p. 211–230.
44 Shibayama, M. Spatial inhomogeneity and dynamic fluctuations of polymer gels. *Macromol. Chem. Phys.* **1998**, *199*, 1–30.

https://doi.org/10.1007/s10118-026-3576-y

45 Pusey, P. N.; Van Megen, W. Dynamic light scattering by non-ergodic media. *Phys. A Stat. Mech. Appl.* **1989**, *157*, 705–741.
46 Joosten, J. G. H.; McCarthy, J. L.; Pusey, P. N. Dynamic and static light scattering by aqueous polyacrylamide gels. *Macromolecules* **1991**, *24*, 6690–6699.
47 Xue, J. Z.; Pine, D. J.; Milner, S. T.; Wu, X. l.; Chaikin, P. M. Nonergodicity and light scattering from polymer gels. *Phys. Rev. A* **1992**, *46*, 6550–6563.
48 Norisuye, T.; Tran-Cong-Miyata, Q.; Shibayama, M. Dynamic inhomogeneities in polymer gels investigated by dynamic light scattering. *Macromolecules* **2004**, *37*, 2944–2953.
49 Jia, D.; Muthukumar, M. Interplay between microscopic and macroscopic properties of charged hydrogels. *Macromolecules* **2020**, *53*, 90–101.
50 Datta, S. S.; Preska Steinberg, A.; Ismagilov, R. F. Polymers in the gut compress the colonic mucus hydrogel. *Proc. Natl. Acad. Sci. U. S. A.* **2016**, *113*, 7041–7046.
51 González-Díaz, E. C.; Varghese, S. Hydrogels as extracellular matrix analogs. *Gels* **2016**, *2*, 20.
52 Raia, N. R.; Jia, D.; Ghezzi, C. E.; Muthukumar, M.; Kaplan, D. L. Characterization of silk-hyaluronic acid composite hydrogels towards vitreous humor substitutes. *Biomaterials* **2020**, *233*, 119729.
53 Bej, R.; Haag, R. Mucus-inspired dynamic hydrogels: synthesis and future perspectives. *J. Am. Chem. Soc.* **2022**, *144*, 20137–20152.
54 Sdobnov, A.; Piavchenko, G.; Bykov, A.; Meglinski, I. Advances in dynamic light scattering imaging of blood flow. *Laser Photonics Rev.* **2024**, *18*, 2300494.
55 Raia, N. R.; Partlow, B. P.; McGill, M.; Kimmerling, E. P.; Ghezzi, C. E.; Kaplan, D. L. Enzymatically crosslinked silk-hyaluronic acid hydrogels. *Biomaterials* **2017**, *131*, 58–67.
56 Zhao, Y. H.; Jie, Y. S.; Xue, Y. C.; Shi, Z. W.; Dong, Y. C.; Muthukumar, M.; Jia, D. Universal law of hierarchical dynamics in gels arising from confluence of local physically dynamic bonds. *Nat. Commun.* **2025**, *16*, 3247.
57 Lee, H.; Kim, J.; Lee, M.; Kang, J. Dynamic bond chemistry in soft materials: bridging adaptability and mechanical robustness. *Chem. Rev.* **2025**, *125*, 11379–11425.
58 Flory, P. J. in *Principles of Polymer Chemistry*, Cornell University Press, **1953**, p. 523–555.

https://doi.org/10.1007/s10118-026-3576-y